The Journal of Immunology

The Influence of Immune Complex-Bearing Follicular Dendritic Cells on the IgM Response, Ig Class Switching, and Production of High Affinity IgG

Yüksel Aydar, Selvakumar Sukumar, Andras K. Szakal and John G. Tew

J Immunol 2005; 174:5358-5366; ;
doi: 10.4049/jimmunol.174.9.5358
http://www.jimmunol.org/content/174/9/5358

The Journal of Immunology is published twice each month by
The American Association of Immunologists, Inc.,
1451 Rockville Pike, Suite 650, Rockville, MD 20852

Print ISSN: 0022-1767 Online ISSN: 1550-6606.

The Influence of Immune Complex-Bearing Follicular Dendritic Cells on the IgM Response, Ig Class Switching, and Production of High Affinity IgG[1]

Yüksel Aydar,[2]* Selvakumar Sukumar,[2]* Andras K. Szakal,[†] and John G. Tew[3]*

It is believed that Ag in immune complexes (ICs) on follicular dendritic cells (FDCs) selects high affinity B cells and promotes affinity maturation. However, selection has been documented in the absence of readily detectable ICs on FDCs, suggesting that FDC-ICs may not be important. These results prompted experiments to test the hypothesis that IC-bearing murine FDCs can promote high affinity IgG responses by selecting B cells after stimulating naive IgM$^+$ cells to mature and class switch. Coculturing naive λ^+ B cells, FDCs, (4-hydroxy-3-nitrophenyl)acetyl-chicken γ-globulin (CGG) + anti-CGG ICs, and CGG-primed T cells resulted in FDC-lymphocyte clusters and production of anti-4-hydroxy-5-iodo-3-nitrophenyl acetyl. Class switching was indicated by a shift from IgM to IgG, and affinity maturation was indicated by a change from mostly low affinity IgM and IgG in the first week to virtually all high affinity IgG anti-4-hydroxy-5-iodo-3-nitrophenyl acetyl in the second week. Class switching and affinity maturation were easily detectable in the presence of FDCs bearing appropriate ICs, but not in the absence of FDCs. Free Ag plus FDCs resulted in low affinity IgG, but affinity maturation was only apparent when FDCs bore ICs. Class switching is activation-induced cytidine deaminase (AID) dependent, and blocking FDC-CD21 ligand-B cell CD21 interactions inhibited FDC-IC-mediated enhancement of AID production and the IgG response. In short, these data support the concept that ICs on FDCs can promote AID production, class switching, and maturation of naive IgM$^+$ B cells, and further suggest that the IC-bearing FDCs help select high affinity B cells that produce high affinity IgG. *The Journal of Immunology,* **2005, 174: 5358–5366.**

Germinal centers (GCs)[4] are a distinctive architectural feature of secondary lymphoid tissues that become apparent after appropriate stimulation with Ag (1–3). The GC reaction is characterized by aggregates of rapidly proliferating B cells in a microenvironment that includes Th cells and follicular dendritic cells (FDCs) bearing immune complexes (ICs) containing the specific Ag (1–6). Major events known to occur in GCs include Ig class switching, somatic hypermutation, selection of somatically mutated B cells with high affinity receptors, production of B memory cells, and production of plasmablasts that home to bone marrow and certain other sites to mature and produce the high affinity Ab responsible for affinity maturation (1, 2, 7–12). An in vitro model of the GC reaction can be studied by coculturing specific B and T cells with FDCs bearing ICs containing specific Ag. B cells in the cocultures cluster around the FDCs, proliferate, and produce specific Abs (13–16). Many GC events including Ig class switching, somatic hypermutation, selection of high affinity B cells, and affinity maturation are challenging to study in vivo. In vitro models that are more amenable to manipulation offer an opportunity to study the role of various cell types, including FDCs and their costimulatory molecules, in a microenvironment representative of the GC.

FDCs are unique accessory cells that trap ICs and serve as a source of Ag for GC-B cells (5, 16, 17), but the extent of their involvement in B cell maturation and differentiation remains to be fully elucidated. Although FDCs represent only 1–2% of all GC cells, their numerous long slender dendrites intertwine and create an extensive network or reticulum that makes them a prominent GC component (18). The extensive network enables FDCs to be in intimate contact with neighboring B cells (90% of GC cells) and T cells (5–10% of GC cells) (5, 18–20). FDCs capture and retain IC using their complement (21, 22) and FcγRs (23, 24) and deliver the Ag in the form of IC-coated bodies (iccosomes) to neighboring B cells for subsequent presentation by the GC-B cell to obtain T cell help (16, 17). In addition, engagement of CD21 in the B cell coreceptor complex by complement-derived FDC-CD21 ligand delivers a critical signal that augments stimulation delivered by engagement of BCR by Ag on FDCs. ICs activate the complement pathway, and C3b and C4b fragments covalently bind to FDCs through thio ester linkages and the IC-bearing FDCs label intensely with Abs reactive with these complement components (25, 26). The C3b component on FDCs degrades to become iC3b, C3d, or C3dg, and these fragments are ligands for complement receptor 2 or CD21. Blockade of CD21 ligand or CD21 in the coreceptor complex virtually eliminates recall Ab responses both in vitro and in vivo (6, 27–29).

It is also widely believed that the ICs on FDCs play a major role in selecting high affinity B cells and promoting affinity maturation. It is reasoned that B cells with high affinity receptors are at a competitive advantage for binding free epitopes of Ags trapped by FDCs. The B cells that succeed in binding Ag are selected to survive, proliferate, and differentiate into plasma cells that produce

Departments of *Microbiology and Immunology and [†]Anatomy and Neurobiology, Immunology Group, Virginia Commonwealth University, Richmond, VA 23298

Received for publication October 13, 2004. Accepted for publication February 23, 2005.

The costs of publication of this article were defrayed in part by the payment of page charges. This article must therefore be hereby marked *advertisement* in accordance with 18 U.S.C. Section 1734 solely to indicate this fact.

[1] This work was supported by National Institutes of Health Grant AI-17142.

[2] Y.A. and S.S. made equal contributions to this study.

[3] Address correspondence and reprint requests to Dr. John G. Tew, Virginia Commonwealth University, Department of Microbiology and Immunology, P.O. Box 980678, Richmond, VA 23298-0678.

[4] Abbreviations used in this paper: GC, germinal center; AID, activation-induced cytidine deaminase; CGG, chicken γ-globulin; FDC, follicular dendritic cell; HSA, human serum albumin; IC, immune complex; NIP, 4-hydroxy-5-iodo-3-nitrophenyl acetyl; NP, (4-hydroxy-3-nitrophenyl)acetyl.

0022-1767/05/$02.00

Ab of high affinity. As the levels of high affinity-specific Ab in serum increase, the well-known phenomenon of affinity maturation becomes apparent. However, the concept that IC-bearing FDCs play a role in this process has been challenged in a system in which B cell selection occurred in the absence of readily detectable ICs on FDCs, suggesting that FDCs and their associated ICs may not be important in selection and affinity maturation (30, 31). These results prompted experiments to test the hypothesis that ICs on FDCs can promote naive IgM^+ B cells to mature, class switch, and preferentially promote high affinity B cells to produce Ab in a culture system in which T cells, B cells, FDCs, Ag, and ICs are readily amenable to manipulation.

The data reported in this work indicate that B cell maturation and affinity maturation were easily detectable in the presence of FDCs bearing appropriate ICs, but these phenomena were minimal to undetectable in the absence of FDCs. B cell maturation was indicated by induction of activation-induced cytidine deaminase (AID), followed by Ig class switching and specific Ab production. Blocking the interaction between FDC-CD21 ligand and B cell CD21 inhibited AID production, Ig class switching, and IgG production. FDCs plus free Ag also resulted in class switching and production of low affinity IgG, although the levels were reduced relative to FDCs plus ICs. Moreover, optimal high affinity IgG responses were only apparent when B cells competed for epitopes of Ag in ICs on FDCs. In short, the present data provide support for the concept that Ag-Ab-C′ complexes on FDCs can promote AID production and class switching by naive IgM^+ GC-B cells, and suggest that the IC-bearing FDCs help select the B cells with high affinity receptors that ultimately produce high affinity IgG.

Materials and Methods

Animals and immunization

Normal 8- to 12-wk-old C57BL/6 mice were purchased from the National Cancer Institute or The Jackson Laboratory. The mice were housed in standard plastic shoebox cages with filter tops and maintained under specific pathogen-free conditions in accordance with Virginia Commonwealth University Animal Care and Use guidelines. Food and water were supplied ad libitum. Chicken γ-globulin (CGG)-primed T cells were obtained after immunization with 20 μg of CGG (Pel-Freez Biologicals) and 5×10^8 heat-killed *Bordetella pertussis* precipitated in aluminum potassium sulfate (A7167; Sigma-Aldrich), as described previously (13, 14). The mice were given a booster immunization 2 wk later with 50 μg of CGG i.p. and by s.c. injection 5 μg of CGG into the front legs and hind footpads.

Abs and reagents

Mouse CD45R (B220) MicroBeads, mouse CD90 (Thy-1.2) MicroBeads, anti-biotin MicroBeads, and MACS LS columns were purchased from Miltenyi Biotec. Biotin-labeled rat anti-mouse κ was purchased from Zymed Laboratories. Alkaline phosphatase-labeled goat anti-mouse IgG (H + L) and alkaline phosphatase-labeled goat anti-mouse IgM were obtained from Kirkegaard & Perry Laboratories. Anti-mouse FDC (FDC-M1) and anti-mouse CD21/CD35 were purchased from BD Pharmingen. The 4-hydroxy-5-iodo-3-nitrophenyl $acetyl_{19}$ (NIP_{19})-OVA (4-hydroxy-3-ioda-5-nitrophenyl acetyl OVA with 19 NIP groups/OVA), NIP_5-OVA (4-hydroxy-3-ioda-5-nitrophenyl acetyl OVA with 5 NIP groups/OVA), and (4-hydroxy-3-nitrophenyl)$acetyl_{30}$ (NP_{30})-CGG were obtained from Biosearch Technologies. Rat anti-mouse CD40 was obtained from Southern Biotechnology Associates. Low-tox-m rabbit complement was purchased from Cedarlane Laboratories. Heat inactivation was accomplished by incubating the complement in a water bath at 56°C for 30 min. NP-CGG anti-CGG ICs were prepared by incubating the Ag and Ab for 2 h at 37°C at final ratio of 1 ng/ml NP-CGG to 6 ng/ml mouse anti-CGG. The anti-CGG was obtained from hyperimmunized mice with anti-CGG IgG levels in excess of 1 mg/ml. In certain experiments, complement-bearing ICs were made using low-tox-m rabbit complement at 1/12 dilution during the 2-h incubation. Anti-CD21/35 was converted into $F(ab')_2$ using the Pierce ImmunoPure $F(ab')_2$ preparation kit (catalogue 44888). Anti-CD23 (clone B3B4) was a kind gift from D. Conrad of our Department of Microbiology and Immunology.

FDC isolation

FDCs were isolated from lymph nodes (axillary, lateral axillary, inguinal, popliteal, mesenteric, and para-aortic) of normal young adult mice, as previously described (13, 14). In brief, 1 day before FDC isolation, the mice were exposed to whole body irradiation to eliminate most T and B cells (1000 rad, using a $Cesium^{137}$ source) (13). Lymph nodes were collected, and each lymph node capsule was opened using two 26-gauge needles; then the lymph nodes were placed in an enzyme mixture consisting of 1 ml of collagenase D (16 mg/ml, C-1088882; Roche), 0.5 ml of DNaseI (5000 U/ml, D-4527; Sigma-Aldrich), and 0.5 ml of DMEM supplemented with 20 mM HEPES, 2 mM glutamine, 50 μg/ml gentamicin, and MEM nonessential amino acids (Invitrogen Life Technologies). After 30 min at 37°C in a CO_2 incubator, the medium and released cells were removed and transferred to a 15-ml conical centrifuge tube containing 5 ml of DMEM with 20% FCS and placed on ice. The remaining tissue was subjected to a second 30-min digestion in a fresh aliquot of enzyme mixture, and the cells were collected as before. Isolated cells were washed and then incubated with a rat anti-mouse FDC-specific Ab (FDC-M1) for 45 min on ice. The cells were washed and incubated with 1 μg of biotinylated anti-rat Ig specific for κ L chain for 45 min on ice. The cells were then incubated with 40 μl of anti-biotin MicroBeads (Miltenyi Biotec) added to 360 μl of MACS buffer for 15–20 min on ice. The cells were layered on a MACS LS column prewetted with 1 ml of MACS buffer and washed with 10 ml of ice-cold MACS buffer. The LS column was removed from the VarioMACS, and the bound cells were released with 10 ml of MACS buffer. Approximately 85–95% of these cells express the FDC phenotype, FDC-$M1^+$, $CD40^+$, CR1 and 2^+, and $Fc\gamma RII^+$ (S. Sukumar and J. Tew, unpublished observations).

Cell cultures for analysis of AID

Lymphocytes (4×10^6) were cocultured with 1.6×10^6 FDCs in 48-well culture plates (Costar) for 2 days at 37°C in a 5% CO_2 atmosphere. The wells contained 1 ml/well complete medium (DMEM supplemented with 10% FCS, 20 mM HEPES, 2 mM glutamine, 50 μg/ml gentamicin, and MEM nonessential amino acids). LPS at 10 ng/ml (L-2387; Sigma-Aldrich) or 100 ng/ml anti-CD40 + 10 ng/ml IL-4 (R&D Systems) were used to stimulate the lymphocytes. Suboptimal levels of LPS, anti-CD40, and IL-4 were used because FDC costimulatory activity was most apparent at suboptimal concentrations of the primary signal. The influence of FDCs was still apparent at higher concentrations of the primary signal, but the differences were smaller and more difficult to study. After 48 h, cells were harvested and lysed using TRIzol (Invitrogen Life Technologies), and total RNA was extracted following the manufacturer's protocol. For experiments described in Fig. 10, λ^+ B cells and CGG-primed T cells and NP-CGG + anti CGG ICs were cultured in the presence or absence of FDCs for 72 h. At the end of 72 h, B cells were isolated using anti-B220 microbeads and the MACS system. Total RNA from 2×10^6 B cells was extracted using TRIzol.

Quantitative RT-PCR analysis

The mRNA levels for AID were measured using quantitative RT-PCR. The primer and probe sequences used for quantitative RT-PCR are listed in Table I. The18S rRNA level was used as an internal control to normalize the expression levels of AID. PCR were performed in 96-well thin-wall PCR plates covered with transparent optical-quality sealing tapes (Bio-Rad). Amplifications were performed using the One Step RT-PCR kit (Applied Biosystems) under the following conditions: 48°C for 30 min (cDNA synthesis), initial denaturation at 95°C for 10 min, followed by 40 cycles of denaturation at 95°C for 15 s and a combined annealing/extension step at 60°C for 1 min. Data analysis was performed using the iCycler iQ software (Bio-Rad). Finally, differences in mRNA expression levels were calculated using the $\Delta\Delta C_T$ method (32). In short, PCR efficiency was first ascertained to be close to 100% by performing multiple standard curves using serial mRNA dilutions. An amplification cycle threshold value (C_T value), defined as the PCR cycle number at which the fluorescence signal crosses an arbitrary threshold, was calculated for each reaction. The fold change between mRNA expression levels was determined as follows: fold change $= 2^{-\Delta\Delta CT}$, where $\Delta\Delta C_T = (C_{T\ GoI} - C_{T\ Hk})$ sample $- (C_{T\ GoI} - C_{T\ Hk})$ control, C_T is the cycle threshold, GoI is the gene of interest, and Hk is the housekeeping gene.

Purification of naive B cells

Single cell suspensions were prepared by grinding lymph nodes from naive mice between the frosted ends of two sterile slides in complete medium (DMEM supplemented with 10% FCS, 20 mM HEPES, 2 mM glutamine, 50 μg/ml gentamicin, and MEM nonessential amino acids). The suspended

Table I. *Primer and probe sequences used in real-time quantitative RT-PCR analysis*

Gene	Primer/Probe	Sequence
AID	Forward	5′-CTACGTGGTGAAGAGGAGAGATAGTG-3′
	Reverse	5′-TGAGATGTAGCGTAGGAACAACAATT-3′
	Probe	5′-FAM-CACCTTCGCAACAAGTCTGGCTGC-TAMRA-3′
18S rRNA	Forward	5′-AAAATTAGAGTGTTCAAAGCAGGC-3′
	Reverse	5′-CCTCAGTTCCGAAAACCAACAA-3′
	Probe	5′-CY5-CGAGCCGCCTGGATACCGCAGC-BHQ-2[a]

[a] BHQ, Black hole quencher.

cells were centrifuged for 5 min at 1000 rpm at 4°C and resuspended in complete medium. The κ plus λ-positive B cells (total B cells) were positively selected using anti-B220-bearing microbeads. Briefly, the lymphocytes were incubated with 40 μl of anti-B220 MicroBeads (diluted 1/10 in MACS buffer) for 15–20 min on ice. The cells were layered on a MACS LS column prewetted with 1 ml of MACS buffer and washed with 10 ml of ice-cold MACS buffer. The LS column was removed from the VarioMACS, and the bound cells were released with 10 ml of MACS buffer, washed, and used as κ plus λ-positive B cells. Anti-NP Abs in C57BL/6 mice predominantly have λ L chains (33, 34), and we reasoned that the NP response would be enhanced if λ-positive naive B cells were enriched in culture. To obtain the λ-positive naive B cells, we removed κ-positive B cells using 10 μg of κ L chain-specific biotinylated rat anti-mouse mAb for 45 min on ice and trapped the κ-positive B cells on a MACS column with anti-biotin MicroBeads (Miltenyi Biotec). We reasoned that B220-positive cells in the flow through would express the λ and they were isolated using anti-B220, as described above. Naive B cells express membrane IgM, and the presence of IgM on our naive B cell population was confirmed by flow cytometry (Fig. 1). In brief, single cell suspensions of lymph node cells from normal mice were triple labeled with FITC B220, PE-conjugated anti-mouse IgM, and biotin-labeled rat anti-mouse λ. The results indicated that ~95% of our B cells expressed κ rather than λ L chain. However, nearly 98% of the cells that expressed λ L chains were IgM positive, which is expected of B cells in the naive state. Serum anti-NIP levels in these donor mice were too low to measure (<1 ng/ml), again supporting the naive nature of the NIP-specific B cells.

Isolation of CGG-primed T cells

CGG-primed lymphocytes were obtained from draining lymph nodes of CGG-immunized mice 1 wk or more after the CGG booster. Lymph nodes were surgically removed and ground between the frosted ends of two sterile slides. The cells were washed and incubated with 40 μl of mouse anti-CD90 (Thy-1.2) MicroBeads (diluted 1/10 in MACS buffer) for 45 min on ice, and then layered on a MACS LS column prewet with 1 ml of MACS buffer and then washed with 10 ml of ice-cold MACS buffer. The LS column was removed from the VarioMACS, and the bound cells were collected as above.

In vitro GC reactions and the anti-NIP Ab response

In vitro GC reactions were set up by coculturing naive λ-positive B cells (10×10^5 cells/ml), FDCs (4×10^5 cells/ml), CGG-primed T cells (5×10^5 cells/ml), with NP-CGG + anti-CGG ICs (100 ng of NP-CGG/well) in 48-well culture plates (Costar). The wells contained 1 ml/well complete medium (DMEM supplemented with 10% FCS, 20 mM HEPES, 2 mM glutamine, 50 μg/ml gentamicin, and MEM nonessential amino acids). ICs were prepared using NP-CGG and anti-CGG serum, and used to stimulate the lymphocytes. The cultures were incubated at 37°C in a 5% CO_2 atmosphere. Supernatant fluids were harvested on days 7 and 14 and were assayed for NIP-specific low and high affinity IgM and IgG Ab using a solid-phase ELISA. Each experimental group was set up in triplicate.

The ELISA for anti-NIP and affinity

The relative affinities of anti-NIP Abs were determined using an ELISA with OVA coupled to NIP at different ratios, respectively, NIP_{19}-OVA and NIP_5-OVA. NIP has higher affinity for anti-NP Abs than NP, and NIP was used for this reason (33, 34). Briefly, flat-bottom 96-well ELISA plates (Falcon; BD Biosciences) were coated with 100 μg/ml NIP_5-OVA or NIP_{19}-OVA in PBS at 4°C overnight. After washing the plates three times with 1× PBS containing 0.1% Tween 20, the plates were blocked with 5% BSA for 2 h at room temperature. Supernatant fluids from the cultures were then added to the plates at a starting dilution of 1/2 for wells with low responses and incubated at 4°C overnight. Alkaline phosphatase-conjugated goat Ab specific for mouse IgM or IgG was added and incubated overnight. Alkaline phosphatase activity was visualized using a *p*NPP phosphatase substrate kit (Kirkegaard & Perry Laboratories), and ODs were determined at 450 nm. Standard curves for IgM or IgG were established by incubating the plates with 100 μg/ml affinity-purified goat anti-mouse IgM or IgG (Sigma-Aldrich). The plates were then washed and incubated with 2-fold dilutions of mouse IgM or IgG (Sigma-Aldrich) starting at 100 ng/ml, and the plates were incubated at 4°C overnight. A standard curve was run on each plate, and concentrations of anti-NIP IgM or IgG Abs were calculated by comparison with standard curves in the linear dose range. The relative affinity of the Abs was indicated by the level of Ab using NIP_{19}-OVA, which measures both high and low affinity anti-NIP, vs NIP_5-OVA, which indicates only high affinity anti-NIP.

Statistical analysis

For analysis of ELISA readings, a *t* test (two-tailed distribution) was used. In some experiments, up to five different comparisons were done, and a *p* value of <0.01 was required to account for multiple comparisons. The $2^{-\Delta\Delta C}{}_T$ method, as described by Livak and Schmittgen (32), was used to analyze real-time quantitative PCR results for the analysis of relative gene expression data

Results

Induction of NIP-specific IgM responses

Stimulation of Ag-specific B cells and class switching takes place in GCs, prompting us to reason that FDCs might enhance IgM responses and Ig class switching. To begin testing, we isolated naive IgM-expressing B cells (Fig. 1), in which a switch from producing IgM to IgG could be easily monitored. NIP-specific Ab responses were initiated in in vitro GCs using λ L chain-expressing B cells (λB cells) from normal mice, carrier-primed T cells (CGG-T cells) from CGG immune mice, FDCs from normal mice, and ICs consisting of NP-CGG anti-CGG. After overnight incubation, FDC-lymphocyte clusters were seen resembling those described by Kosco et al. (13), and these clusters persisted through

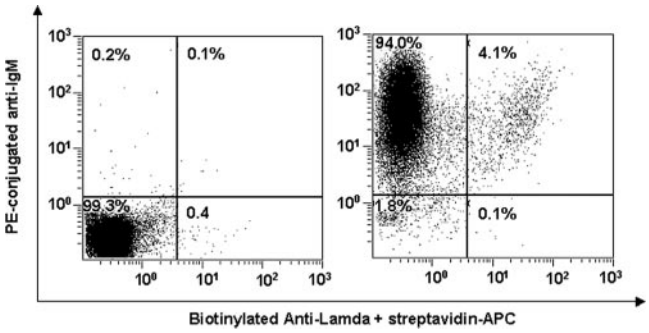

FIGURE 1. Flow cytometric analysis of the naive B cell population. $B220^+$ cells were isolated from lymph nodes of normal mice using MACS technology and then labeled with FITC-conjugated B220, PE-conjugated anti-IgM, and biotinylated anti-λ, which was then visualized with streptavidin-APC. The B220-positive cells were gated for analyses of IgM- and λ-expressing B cells (*right panel*), and the isotype controls for anti-IgM and anti-λ are included in the *left panel*. Percentages are indicated in the squares, and these results are representative of three experiments of this type.

the 14 days of culture. We reasoned that naive B cells would initially produce IgM and, as indicated in Fig. 2*A* (fourth □), over 120 ng of IgM anti-NIP accumulated by day 7 using this combination of immunogen and cells. Anti-NIP is largely derived from λ-bearing B cells, and the use of purified λB cells was helpful, as naive B cells containing κ and λ B cells (κ + λB cells) in normal amounts (~95% κ) did produce IgM anti-NIP (~20 ng/ml), but not as well as the λ-bearing cells (Fig. 2*A*, □, 3 vs 4). Use of ICs that could be trapped and presented to B cells by FDCs was also important, as free Ag (NP-CGG) did not work as well as ICs (Fig. 2*A*, □, 4 vs 5). Also note that if either immunogen (Ag or ICs) or FDCs were missing or if OVA-primed T cells were substituted for CGG-primed T cell, the NIP-specific IgM response was typically undetectable. The low IgM response obtained with ICs in the absence of FDCs at day 7 in this experiment is not a consistent observation. The culture medium was replaced on day 7, and some IgM accumulated in the second week (Fig. 2*A*, ■), but the levels were low compared with anti-NIP IgM in the first week. As expected, the assay using NIP-5 to detect high affinity Ab indicated very little IgM anti-NIP was produced even in the presence of FDCs (Fig. 2*B*).

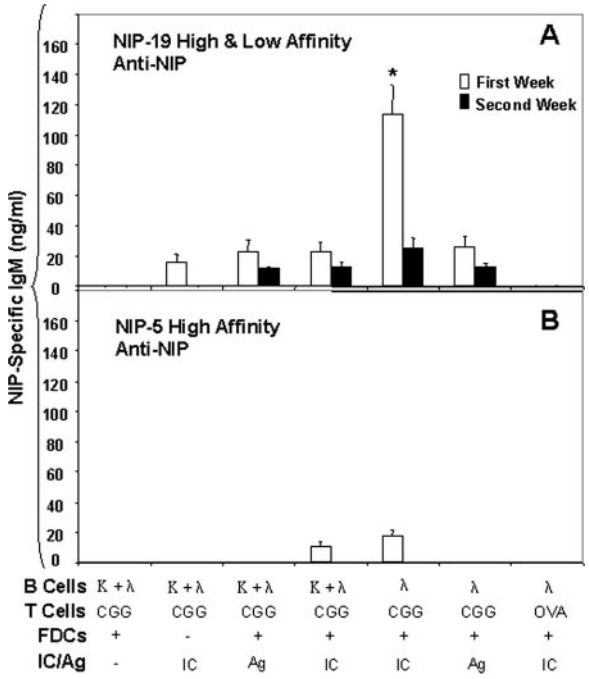

FIGURE 2. FDCs promote the production of NP-specific IgM in cocultures with naive B cells. Naive λ^+ B cells and FDCs were isolated from naive C57BL/6 mice, and CCG-primed T cells were isolated from C57BL/6 mice immunized with CGG. ICs were prepared using NP-CGG and anti-CGG hyperimmune mouse serum. A total of 1×10^6 naive λ^+ B cells, 0.5×10^6 CGG-primed T cells, and 0.4×10^6 FDCs was cocultured in the presence or absence of 100 ng of NP-CGG in ICs or as free Ag. Culture supernatant fluids were collected at day 7 and replaced with fresh medium. NIP-specific IgM accumulated in supernatant fluids at days 7 and 14 of cell culture were measured using ELISA. All data are representative of three independent experiments. *A*, Shows total NIP-specific IgM; *B*, shows high affinity NIP-specific IgM Abs. □, NIP-specific IgM Abs generated in the first week; ■, NIP-specific IgM generated in the second week. Affinity maturation of NIP-specific IgM was estimated by comparing the amount of NIP-specific IgM bound to NIP_{19}-OVA for total and to NIP_5-OVA for high affinity NIP-specific IgM Abs. The error bars around the mean represent the SEM for replicate cultures. *, Indicates the response is significantly elevated ($p < 0.01$) over all other groups in the first week.

Ig class switching and the NIP-specific IgG response

The IgG anti-NIP response was studied in the same cultures described in Fig. 2 for the NIP-specific IgM. The need for λB cells, CGG-primed T cells, FDCs, and NP-CGG anti-CGG ICs was the same for optimal IgG production and was apparent as it was for IgM (Fig. 3*A*, third □ and third ■). The anti-NIP IgG that accumulated in the first week in Fig. 3*A* was about one-half the level of anti-NIP IgM in Fig. 2*A* (~60 ng/ml IgG vs 120 ng/ml IgM; $p <$ 0.01). However, these relationships were reversed in the second week with over 140 ng/ml IgG vs only 20 ng/ml IgM (■ in Fig. 2*A* vs 3*A*; $p < 0.01$). In short, the Ig isotype produced switched from predominantly IgM in the first week to predominantly IgG in the second week.

Affinity maturation and the importance of ICs

In contrast with IgM, large amounts of IgG were apparent when NIP-5 was used to detect high affinity Ab. Of major interest was that only ~30–50% of the IgG made in the first week was of high affinity (NIP-5 vs NIP-19). However, almost all of the IgG made in the second week was of high affinity (Fig. 3*B*). This is consistent with selection of high affinity B cells and selective stimulation of these cells to produce the high affinity IgG associated with affinity maturation. Furthermore, affinity maturation was only observed

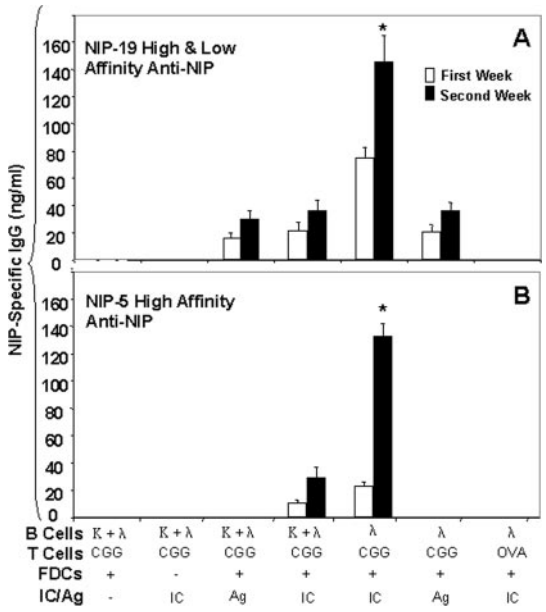

FIGURE 3. FDCs promote production of NP-specific IgG and affinity maturation in cocultures with naive B cells. The same cell cultures used to study production of NIP-specific IgM in Fig. 1 were used to study total and high affinity NIP-specific IgG Abs. Culture supernatant fluids were collected at day 7 and replaced with fresh medium. NIP-specific IgG accumulated in supernatant fluids at days 7 and 14 after cell culture were measured using ELISA. All data are representative of three independent experiments. *A*, Shows total NIP-specific IgG; *B*, shows high affinity NIP-specific IgG Abs. □, NIP-specific IgG Abs generated in the first week; ■, NIP-specific IgG Abs generated in the second week. Class switching from IgM to IgG was estimated by comparing the amount of IgM and IgG generated in the first vs the second week. Affinity maturation of NIP-specific IgG was estimated by comparing the amount of NIP-specific IgG bound to NIP_{19}-OVA and NIP_5-OVA. The difference between NIP-specific IgG bound to NIP_{19}-OVA and NIP-specific IgG bound to NIP_5-OVA reflects the affinity maturation of NIP-specific IgG Abs. The error bars around the mean represent the SEM for replicate cultures. *, Indicates the response is significantly elevated ($p < 0.01$) over all other groups in the corresponding week.

when Ag was in the form of ICs that would be trapped and presented to B cells by FDCs. Free Ag (NP-CGG) that should engage BCR efficiently did stimulate low affinity IgG (Fig. 3*A*, first and fourth ■), but did not stimulate detectable levels of high affinity IgG (Fig. 3*B*). In the absence of FDCs, ICs engage BCR and FcγRII, leading to ITIM activation, SHIP phosphorylation, and a lack of responsiveness. Trapping the Ig-Fc by high levels of FcgRII on FDCs minimizes engagement of FcgRII on the B cell and facilitates a productive IgG response (35, 36). Thus, we reason the only ICs capable of stimulating B cells for a productive IgG response would be those trapped by the FDCs.

Importance of CD21-CD21 ligand interactions for IgM responses and class switching

Interaction between FDC-CD21 ligand and CD21 in the B cell coreceptor complex (CD21/CD19/CD81) is critical for FDC-associated Ag to stimulate optimal recall responses (6, 28). IgM responses in CD21/CD19 knockout mice are also depressed (37), prompting us to reason that blocking signals to B cells delivered via FDC-CD21 ligand-CD21 interactions might inhibit IgM production and class switching. The results in Fig. 4 indicate that anti-CD21 inhibited the IgM response and, consistent with a reduction in class switching, the IgG response was dramatically reduced (>90%) at its peak in the second week. The diminished IgG response was not simply attributable to a loss of B cells in the absence of CD21 ligand-CD21 interactions because the number of B cells persisting in cultures treated with anti-CD21 was not significantly lower than the B cell number with the isotype control. We also considered the possibility that the Fc portion of the intact IgG-binding B cell-CD21 could engage B cell-FcγRII and lead to ITIM activation, and thus explain the reduced Ab response with anti-CD21. However, if the anti-CD21 is simply blocking the receptor, then anti-CD21 $F(ab')_2$ should work as well as the intact Ab, and this proved to be the case (Fig. 5).

Both FDCs and B cells express CD21 and CD23. CD23 is a ligand for CD21 in the human system (38), raising the possibilities that anti-CD21 could influence the activity of FDC or that FDC-CD23 could engage B cell CD21 and provide a signal to the B cells. However, treating FDCs with anti-CD21 did not inhibit their activity, and treating B cells and FDCs with anti-CD23 did not have any detectable effect (Fig. 5).

We also sought to determine whether increasing CD21 ligand levels on FDCs would increase class switching and production of high affinity NIP-specific IgG. As illustrated in Fig. 6, treating ICs with complement to enhance CD21 ligand levels on the FDCs did not increase the anti-NIP response. This is consistent with previous data in which additional CD21 ligand did not increase the murine anti-OVA response in normal mice (39). However, in aged mice, the level of CD21 ligand covalently bound to the FDCs appears to be low and the addition of rabbit complement to increase levels of FDC-CD21 ligand on aged FDCs improved accessory activity and the B cell responses (39).

AID expression and the influence of FDCs

AID is important in class switching and is expressed in GC-B cells and in B cells undergoing class switch recombination in vitro (40–42). We reasoned that FDCs may help regulate AID expression by GC-B cells and sought to test this hypothesis. Expression of AID mRNA can be detected in lymphocytes stimulated with LPS, or with IL-4 + anti-CD40, in which a large proportion of B cells is stimulated with these polyclonal B cell activators. We reasoned

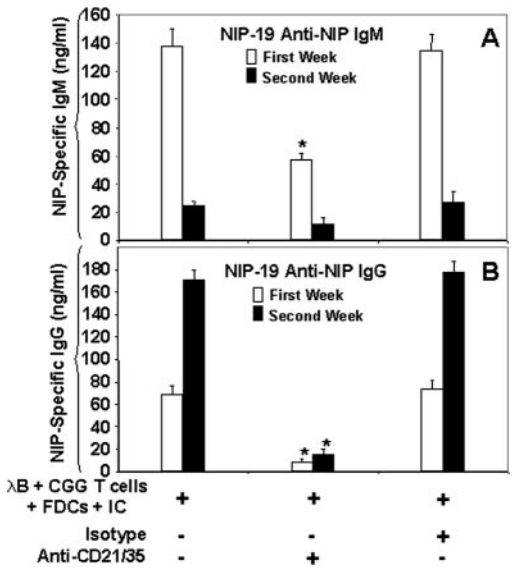

FIGURE 4. Inhibition of the IgM response and Ig class switching by hindering FDC-CD21 ligand-B cell-CD21 interactions with anti-CD21. The cell cultures were incubated with CD21/35 (7G6) or isotype control (used at 10 μg/ml). Culture medium was replaced on day 7, and NIP-specific IgM (*A*) and IgG (*B*) accumulated in supernatant fluids on 7 and 14 days were measured using the NIP_{19}-OVA ELISA for total anti-NIP. The samples in each group were done in triplicate, and the result is representative of three experiments of this type. The error bars around the mean represent the SEM for replicate cultures. ∗, Indicates the response was significantly suppressed ($p < 0.01$) when compared with the corresponding groups without anti-CD21.

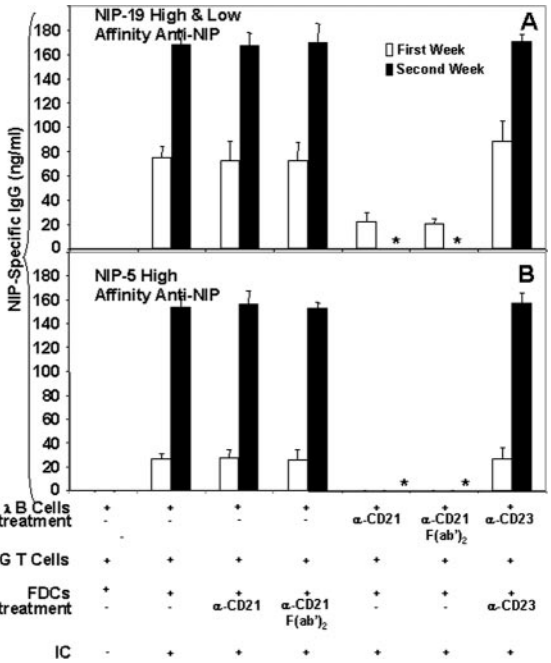

FIGURE 5. Inhibition of the NIP-specific IgG responses by hindering FDC-CD21 ligand-B cell-CD21 interactions with anti-CD21 or $F(ab')_2$ anti-CD21, but not by anti-CD23. B cells or FDCs were incubated with intact anti-CD21/35 (at 10 μg/ml), $F(ab')_2$ of anti-CD21/35 (at 5 μg/ml), or anti-CD23 (B3B4) (at 10 μg/ml) for 2 h, and then washed and placed in culture. Culture medium was replaced on day 7, and the NIP-specific IgG that accumulated in supernatant fluids on 7 and 14 days was measured using the NIP_{19}-OVA (*A*) or NIP_5-OVA (*B*) ELISA. The error bars around the mean represent the SEM for replicate cultures. ∗, Indicates the response was significantly suppressed ($p < 0.01$) when compared with the corresponding control group without anti-CD21.

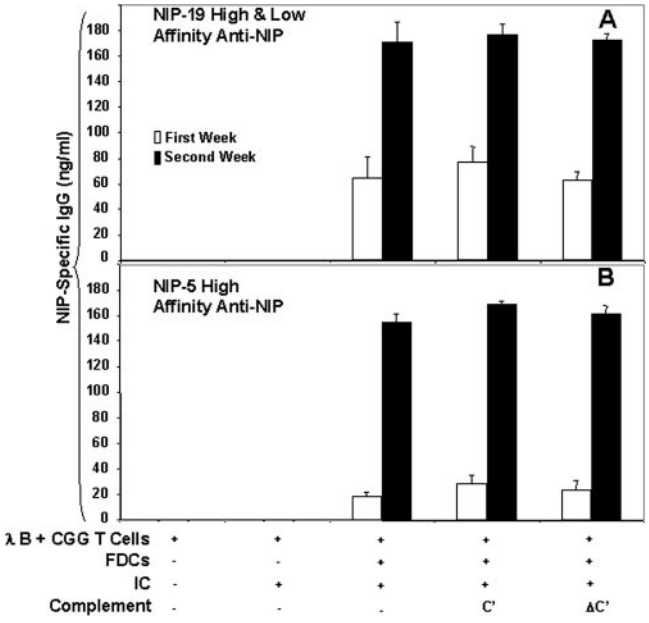

FIGURE 6. Incubating ICs with complement to deposit more CD21 ligand on FDCs did not enhance the anti-NIP response. NP-CGG anti-CGG IC with or without complement were prepared by incubating the Ag and Ab for 2 h at 37°C in the absence of complement or in the presence of low-tox-m rabbit complement (C′) or complement heat inactivated at 56°C for 30 min (Δ C′). NIP specific Ab (IgG) was measured using NIP_{19}-OVA (*A*) and NIP_5-OVA (*B*) after 7 and 14 days of culture. The error bars around the mean represent the SEM for replicate cultures.

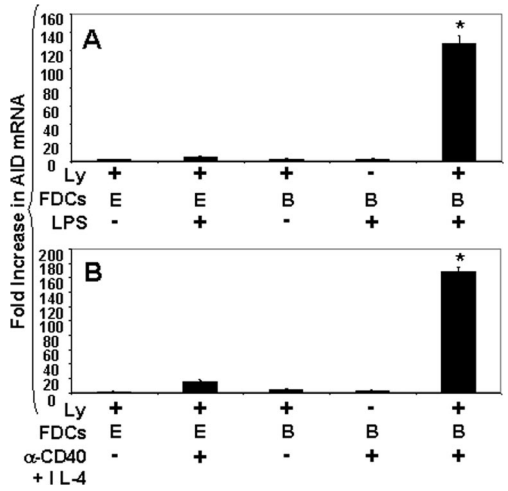

FIGURE 7. FDCs enhanced AID mRNA expression in stimulated B cells. *A*, Lymphocytes were stimulated with suboptimal levels of LPS (10 ng/ml) and were cocultured in the absence or presence of FDCs. After 48 h, cells were harvested and lysed using TRIzol, and total RNA was extracted and amplified with RT-PCR. FDCs were added to the cultures either at the beginning (indicated by the letter B after FDCs) to provide costimulation or at the end (indicated by the letter E after FDCs) of the culture so that FDC-RNA was constant in all analyses. Data are the mean ± SD from five experiments. *B*, This is a replicate of *A*, except LPS was replaced with suboptimal levels of IL-4 (10 ng) + anti-CD40 (100 ng) to stimulate the B cells. ∗, Indicates the response is significantly elevated ($p < 0.01$) over all other groups.

that costimulation of B cells with FDCs might amplify AID mRNA. To test this, quantitative real-time PCR was used to determine the levels of AID mRNA. Suboptimal amounts of LPS (10 ng), IL-4 (10 ng), and anti-CD40 (100 ng) were used to stimulate low levels of AID in the lymphocytes. FDCs were added either at the beginning to provide costimulation or at the end of the culture, so that mRNA coming from the FDCs would be constant in all cultures. The AID mRNA level in normal lymphocytes was defined as 1-fold to compare the effect of LPS, or IL-4 + anti-CD40 treatment alone or in the presence of FDCs. Analysis with RT-PCR indicated that LPS increased AID in the lymphocyte population ~8-fold and FDCs ~2-fold (Fig. 7*A*). However, the combination of FDCs with LPS was synergistic, and AID mRNA expression increased 130-fold (Fig. 7*A*). Results with IL-4 + anti-CD40 were similar. The combination of FDCs with IL-4 + anti-CD40 resulted in AID mRNA levels up 180-fold vs 3-fold with FDCs and 18-fold with IL-4 + anti-CD40 (Fig. 7*B*).

No significant AID mRNA was found when FDCs alone were stimulated with LPS or anti-CD40 + IL-4, suggesting that B cells were the source of the mRNA when FDCs and B cells were cultured together (Fig. 7). This was confirmed by isolating mRNA from B cells purified after the 2-day culture period using B220 microbeads with the MACS system (Fig. 8). Note that nearly all of AID mRNA was in the B cell fraction; while the flow through fraction did contain detectable activity, it also contained some contaminating B cells, which most likely accounts for this AID mRNA. Furthermore, the increased AID activity in B cells did not appear to be simply attributable to increased B cell survival or proliferation caused by FDCs because the same number of B cells (2×10^6) was used to obtain the mRNA, and 18S rRNA was used as an internal loading control. Thus, the level of AID mRNA per B cell was elevated when B cells were cultured in the presence of FDCs.

Role of CD21-CD21 ligand interactions in AID expression and class switching

The reduction in class switching observed when CD21 ligand-CD21 interactions were blocked prompted us to reason that the interaction between FDC-CD21 ligand and B cell-CD21 might signal through the coreceptor complex and help regulate expression of AID. To test this, anti-CD21/35 was used to interrupt FDC-CD21 ligand-B cell-CD21 interactions and the level of AID expression was reduced ~90%, indicating this interaction is playing a role (Fig. 9).

Importance of ICs and CD21 ligand for FDC-mediated enhancement of AID responses

A major goal of the present study was to determine whether ICs contribute to the ability of FDCs to promote optimal high affinity Ab responses. Given the importance of FDC-ICs in promoting class switching and affinity maturation, we sought to determine whether ICs and CD21 ligand-CD21 interactions were important in FDC-mediated enhancement of AID expression in the NP-CGG system. The small number of B cells responding to NP-CGG makes study of AID regulation more challenging. However, it was possible to detect FDC-mediated enhancement of AID mRNA when 2×10^6 purified B cells were used for RNA purification after 72 h of culture (Fig. 10). Note that NP-CGG anti-CGG ICs stimulated enhancement, while NP-CGG failed to stimulate detectable enhancement. Furthermore, anti-CD21/35 inhibited the Ag-stimulated response in the same fashion as was observed in studies of B cells stimulated with polyclonal activators.

Discussion

Binding of Ag to BCR initiates activation of Ag-specific B cells, resulting in proliferation and differentiation into Ab-secreting plasma cells or B memory cells. Important events leading to

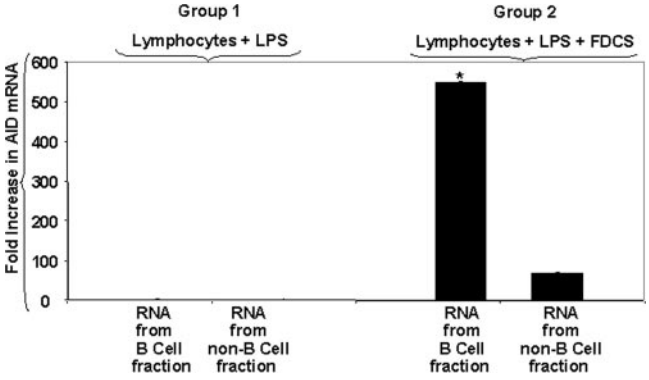

FIGURE 8. B cells express AID, and FDCs promote AID expression per B cell. Lymph node cells were cocultured with LPS (10 ng/ml) (group 1) or LPS + FDC (group 2) for 48 h, as indicated by brackets above the graph. After the 48-h period, the B cells were then separated from all other cell types using B220-coated microbeads into positively selected B cells ($B220^+$ cells) and non-B cells in the flow through fraction (B220-depleted cells with or without FDCs). The difference in B cells in group 1 vs 2 is that B cells in group 2 were in the presence of FDCs during the 48-h culture period. The mRNA for each bar was obtained from 2×10^6 B cells or non-B cells. The error bars around the mean represent the SEM for replicate cultures. *, Indicates the response is significantly elevated ($p < 0.01$) over all other groups.

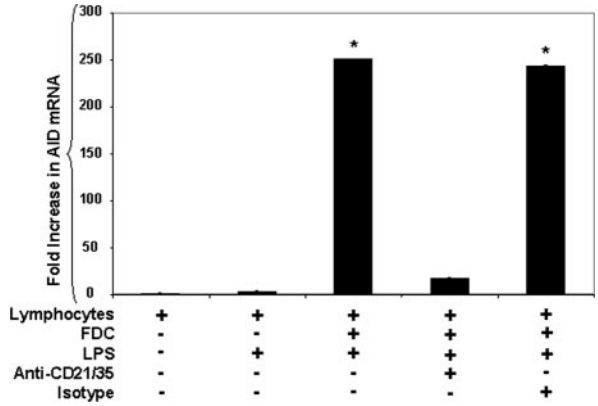

FIGURE 9. Inhibition of AID mRNA production by blocking B cell-CD21 with specific Ab to hinder FDC-CD21 ligand-B cell-CD21 interactions. Lymphocytes stimulated with LPS (10 ng/ml) were cocultured with FDCs in the presence or absence of anti-CD21/35 (10 μg/ml). After 48 h, the cells were harvested and lysed using TRIzol, and the total RNA was extracted and amplified with RT-PCR. The error bars around the mean represent the SEM for replicate cultures. The columns with * were not different from each other, but were significantly elevated ($p < 0.01$) over all other groups.

plasma cells and memory cells take place in GCs in which networks of FDCs are located (1, 2, 8, 12, 18, 43). FDC trap ICs and provide Ag in the form of iccosomes for B cells to process and present to T cells to obtain help, and FDCs provide costimulatory signals that enhance B cell proliferation and Ab production. FDC-CD21 ligand is a costimulatory molecule that engages CD21 in the B cell coreceptor complex and works in combination with FDC-Ag-BCR interactions to achieve optimal signaling and Ab production (6, 18, 28). The consequences of these FDC activities are thought to include H chain class switching (10, 44), formation of memory B cells (1, 45), and selection of high affinity B cell clones for survival (43, 46). Some of these high affinity B cells then differentiate and produce the high affinity Ab that is associated with affinity maturation (11, 16). The data reported in this work demonstrate that optimal class switching and affinity maturation only occurred when IC-bearing FDCs were present.

The concept that IC-bearing FDCs play a role in selection and processes leading to affinity maturation has been challenged using a system in which V gene region hypermutation and mutant B cell selection occurred in the absence of detectable ICs on FDCs (30, 31). Nevertheless, it should be appreciated that the inability to detect Ag persisting on FDCs does not mean it is not present. In the 1960s and 70s, it was difficult to persuade skeptics that intact Ag actually persisted on FDCs for months. Enzyme detection systems, including methods similar to those used in the study by Hannum et al. (30), were not sensitive enough in our hands to detect human serum albumin (HSA) persisting on FDCs after a few weeks in vivo. However, use of ^{125}I-labeled HSA revealed that picogram levels of HSA did persist and that it maintained its original m.w. and its ability to be recognized by specific Ab after 12 wk in mice (47). Furthermore, in lymph node fragments with ^{125}I-labeled Ag persisting on FDCs, 2–4 pg of HSA (100–150 cpm) was sufficient to induce a detectable specific anti-HSA response (48) (see Table IV in Ref. 48), and in other experiments we have been able to detect specific Ab by challenging with FDCs bearing a picogram of persisting Ag (J. Wu and J. Tew, unpublished observations). In short, bioassays for persisting Ag are extremely sensitive, suggesting that tiny amounts of Ag persisting on FDCs can have remarkable biological activity. The fact that Ag was not detected on FDCs with the immunohistochemical approach used by Hannum et al. (30) does not rule out the possibility that some Ag did persist and that FDC-associated Ag did select the mutated B cells.

In the present study, we sought to determine whether FDCs bearing ICs of the appropriate specificity could promote the production of high affinity IgG responses starting with naive IgM^+ B cells. To get a high affinity IgG response, the B cells would need to engage Ag, clonally expand, and class switch, and the high affinity B cells that ultimately produce the high affinity IgG would need to be selected for expansion and Ab production. Class switching and affinity maturation were easily detectable in the presence of FDCs bearing appropriate ICs, but neither phenomenon was detected in the absence of FDCs. The minimal anti-NIP response in cultures stimulated with ICs in the absence of FDCs most likely relates to two problems. First, B cells do not survive well in cultures in the absence of FDCs, and most lymphocytes are dead by the end of 14 days (15). Second, in the absence of FDCs, ICs engage both BCR and B cell FcγRII, and an inhibitory ITIM signal is delivered that minimizes Ab production (35, 36). Trapping Ig-Fc by high levels of FcγRII on FDCs minimizes engagement of FcγRII on B cells and promotes Ig production. We think it is relevant that free Ag plus FDCs, which could provide a variety of trophic factors, did result in a detectable IgG response, but it was consistently of low affinity. Affinity maturation was only apparent when FDCs were allowed to bind ICs and the B cells were forced to compete for Ag trapped in the ICs on the FDCs. Free Ag would engage the Ag receptor on the B cells without difficulty, and competition for epitopes of Ag in the Ag-Ab complexes on FDCs would not be required for stimulation. In addition, these B cells would not simultaneously engage the B cell coreceptor complex with the CD21 ligand that decorates the FDCs. In short, the present data are consistent with the concept that Ag-Ab-C′ complexes on FDCs can serve to select B cells with high affinity receptors that ultimately produce the high affinity IgG Ab.

The precise molecular events associated with isotype switching and affinity maturation in mouse and human are of major interest. Cell culture models that mimic the GC reaction and generate Ag-specific high affinity IgG independent of exogenous mitogens should be helpful in such studies. In the present study, a sensitive

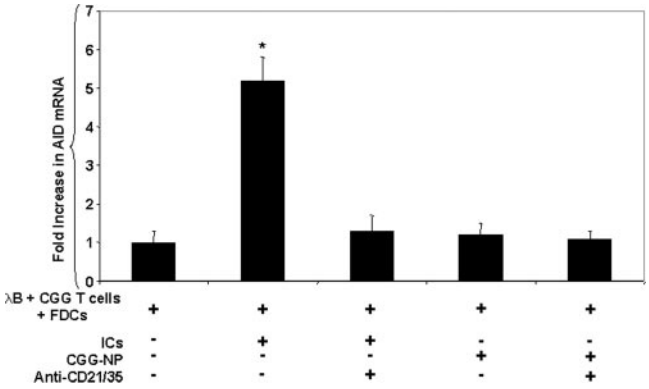

FIGURE 10. Inhibition of AID mRNA production by blocking B cell-CD21 with specific Ab to hinder FDC-CD21 ligand-B cell-CD21 interactions in NIP-stimulated B cells. λ^+ naive B cells, CGG-primed T cells, and FDCs were cocultured with NP-CGG + anti-CGG ICs or NP-CGG to stimulate an immune response. In two groups, the B cells were preincubated for 2 h with anti CD21/35 to block B cell CD21. After 78 h, the B cells were then separated from all other cell types using B220-coated microbeads into positively selected B cells ($B220^+$ cells). The mRNA for each bar was obtained from 2×10^6 B cells. The error bars around the mean represent the SEM for replicate cultures. *, Indicates the response is significantly elevated ($p < 0.01$) over all other groups.

and reproducible culture system was established in which ICs (NP-CGG + anti-CGG) were used to stimulate naive B cells cocultured with FDCs and CGG-primed T cells. The results demonstrate that coculture of naive B cells, CGG-primed T cells, NP-CGG + anti-CGG ICs, and FDCs can trigger the in vitro production of anti-NP Abs. Anti-NP Abs in C57BL/6 mice predominantly express λ L chains, and NIP has higher affinity for anti-NP Abs (33, 34). Therefore, we purified λ-positive naive B cells to enrich for the NP response and coated the ELISA plates with NIP-OVA to measure the anti-NP response. In brief, our results suggest that: 1) λ-positive naive B cells yielded better responses than unselected naive B cells in which B cells expressing κ L chains predominated; 2) ICs were more stimulatory than free Ag, and the ICs were important to get high affinity IgG; 3) primed T cells were essential for the NP response; and 4) FDCs increased class switching and production of high affinity IgG to easily detectable levels. The results obtained using this model further underline a role for FDCs and FDC-trapped ICs for class switching and affinity maturation.

Class switching and up-regulation of AID in lymphocytes may be demonstrated after stimulation with anti-CD40, IL-4, LPS, and TGF-β (40, 49). The ability of such stimulators to up-regulate AID expression in B cells was confirmed in our experiments. Furthermore, addition of FDCs with these primary stimulators resulted in increased AID mRNA levels ~150-fold over background. This is consistent with the observation that AID is heavily expressed in GC-B cells adjacent to FDCs in follicles of lymph nodes and tonsils (40, 41). Our results also indicated that resting FDCs or FDCs stimulated with LPS or anti-CD40 + IL-4 did not have AID activity, thus confirming and extending the observation that AID appeared to be exclusively expressed by GC-B cells (40, 41, 50). Furthermore, FDCs and NP-CGG anti-CGG ICs stimulated enhancement of AID in B cells, while FDCs and NP-CGG failed to stimulate detectable enhancement, further emphasizing the importance of ICs on FDCs.

The ability of FDC to up-regulate AID mRNA was costimulatory in nature, and a primary signal that could be delivered by anti-CD40 and IL-4, LPS, or IC was required. FDC-CD21 ligand appears to play a role in providing the costimulatory effect because blocking B cell-CD21 in the coreceptor complex virtually eliminated FDC activity (Figs. 9 and 10). This observation is consistent with studies indicating that simultaneous stimulation of the B cell line, BL2, with Abs to CD19, CD21, and IgM induces specific V gene mutations, and that generation of memory B cells is impaired in $CD21^{-/-}$ mice (42, 51, 52). The present results also extend the observation that optimal IgG responses require that FDC-CD21 ligand be able to engage B cell-CD21, and the data in Fig. 4 suggest that the interaction helps regulate switching to the IgG isotype.

Affinity maturation is thought to occur as a consequence of selection of high affinity B cells for survival and activation as a result of engaging ICs on FDCs. A major source of high affinity B cells in GCs comes as a consequence of somatic hypermutations (2, 7, 9, 10). We reason that the high affinity anti-NP IgG obtained in our cultures is most likely generated as a consequence of somatic hypermutation, and studies are planned to determine the frequency and distribution of mutations in Ig genes in the presence and absence of FDCs incubated with Ag or ICs in our in vitro cell cultures.

Disclosures

The authors have no financial conflict of interest.

References

1. MacLennan, I. C. 1994. Germinal centers. *Annu. Rev. Immunol. 12:117.*
2. Kelsoe, G. 1996. The germinal center: a crucible for lymphocyte selection. *Semin. Immunol. 8:179.*
3. McHeyzer-Williams, M. G. 2003. B cells as effectors. *Curr. Opin. Immunol. 15:354.*
4. Szakal, A. K., and M. G. Hanna, Jr. 1968. The ultrastructure of antigen localization and virus-like particles in mouse spleen germinal centers. *Exp. Mol. Pathol. 8:75.*
5. Tew, J. G., M. H. Kosco, G. F. Burton, and A. K. Szakal. 1990. Follicular dendritic cells as accessory cells. *Immunol. Rev. 117:185.*
6. Tew, J. G., J. Wu, M. Fakher, A. K. Szakal, and D. Qin. 2001. Follicular dendritic cells: beyond the necessity of T-cell help. *Trends Immunol. 22:361.*
7. Berek, C. 1993. Somatic mutation and memory. *Curr. Opin. Immunol. 5:218.*
8. Camacho, S. A., M. H. Kosco-Vilbois, and C. Berek. 1998. The dynamic structure of the germinal center. *Immunol. Today 19:511.*
9. Li, Z., C. J. Woo, M. D. Iglesias-Ussel, D. Ronai, and M. D. Scharff. 2004. The generation of antibody diversity through somatic hypermutation and class switch recombination. *Genes Dev. 18:1.*
10. Liu, Y. J., F. Malisan, O. de Bouteiller, C. Guret, S. Lebecque, J. Banchereau, F. C. Mills, E. E. Max, and H. Martinez-Valdez. 1996. Within germinal centers, isotype switching of immunoglobulin genes occurs after the onset of somatic mutation. *Immunity 4:241.*
11. Rao, S. P., K. A. Vora, and T. Manser. 2002. Differential expression of the inhibitory IgG Fc receptor FcγRIIB on germinal center cells: implications for selection of high-affinity B cells. *J. Immunol. 169:1859.*
12. Tew, J. G., R. M. DiLosa, G. F. Burton, M. H. Kosco, L. I. Kupp, A. Masuda, and A. K. Szakal. 1992. Germinal centers and antibody production in bone marrow. *Immunol. Rev. 126:1.*
13. Kosco, M. H., E. Pflugfelder, and D. Gray. 1992. Follicular dendritic cell-dependent adhesion and proliferation of B cells in vitro. *J. Immunol. 148:2331.*
14. Wu, J., D. Qin, G. F. Burton, A. K. Szakal, and J. G. Tew. 1996. Follicular dendritic cell (FDC) derived Ag and accessory activity in initiation of memory IgG responses in vitro. *J. Immunol. 157:3404.*
15. Qin, D., J. Wu, G. F. Burton, A. K. Szakal, and J. G. Tew. 1999. Follicular dendritic cells mediated maintenance of primary lymphocyte cultures for long-term analysis of a functional in vitro immune system. *J. Immunol. Methods 226:19.*
16. Tew, J. G., J. Wu, D. Qin, S. Helm, G. F. Burton, and A. K. Szakal. 1997. Follicular dendritic cells and presentation of antigen and costimulatory signals to B cells. *Immunol. Rev. 156:39.*
17. Kosco, M. H., A. K. Szakal, and J. G. Tew. 1988. In vivo obtained antigen presented by germinal center B cells to T cells in vitro. *J. Immunol. 140:354.*
18. Szakal, A. K., M. H. Kosco, and J. G. Tew. 1989. Microanatomy of lymphoid tissue during the induction and maintenance of humoral immune responses: structure function relationships. *Annu. Rev. Immunol. 7:91.*
19. Nieuwenhuis, P., and D. Opstelten. 1984. Functional anatomy of germinal centers. *Am. J. Anat. 170:421.*
20. Schriever, F., A. S. Freedman, G. Freeman, E. Messner, G. Lee, J. Daley, and L. M. Nadler. 1989. Isolated human follicular dendritic cells display a unique antigenic phenotype. *J. Exp. Med. 169:2043.*
21. Klaus, G. G. B., and J. H. Humphrey. 1977. The generation of memory cells. I. The role of C3 in the generation of B memory cells. *Immunology 33:31.*

22. Papamichail, M., C. Gutierrez, P. Embling, P. Johnson, E. J. Holborrow, and M. B. Pepys. 1975. Complement dependence of localization of aggregated IgG in germinal centers. *Scand. J. Immunol. 4:343*.
23. Yoshida, K., T. K. Van den Berg, and C. D. Dijkstra. 1993. Two functionally different follicular dendritic cells in secondary lymphoid follicles of mouse spleen, as revealed by CR1/2 and FcRγII-mediated immune-complex trapping. *Immunology 80:34*.
24. Qin, D., J. Wu, K. A. Vora, J. V. Ravetch, A. K. Szakal, T. Manser, and J. G. Tew. 2000. Fcγ receptor IIB on follicular dendritic cells regulates the B cell recall response. *J. Immunol. 164:6268*.
25. Taylor, P. R., M. C. Pickering, M. H. Kosco-Vilbois, M. J. Walport, M. Botto, S. Gordon, and L. Martinez-Pomares. 2002. The follicular dendritic cell restricted epitope, FDC-M2, is complement C4; localization of immune complexes in mouse tissues. *Eur. J. Immunol. 32:1888*.
26. Gajl-Peczalska, K. J., A. J. Fish, H. J. Meuwissen, D. Frommel, and R. A. Good. 1969. Localization of immunological complexes fixing β1C (C3) in germinal centers of lymph nodes. *J. Exp. Med. 130:1367*.
27. Hebell, T., J. M. Ahearn, and D. T. Fearon. 1991. Suppression of the immune response by a soluble complement receptor of B lymphocytes. *Science 254:102*.
28. Qin, D., J. Wu, M. C. Carroll, G. F. Burton, A. K. Szakal, and J. G. Tew. 1998. Evidence for an important interaction between a complement-derived CD21 ligand on follicular dendritic cells and CD21 on B cells in the initiation of IgG responses. *J. Immunol. 161:4549*.
29. Fakher, M., J. Wu, D. Qin, A. K. Szakal, and J. G. Tew. 2001. Follicular dendritic cell accessory activity crosses MHC and species barriers. *Eur. J. Immunol. 31:176*.
30. Hannum, L. G., A. M. Haberman, S. M. Anderson, and M. J. Shlomchik. 2000. Germinal center initiation, variable gene region hypermutation, and mutant B cell selection without detectable immune complexes on follicular dendritic cells. *J. Exp. Med. 192:931*.
31. Haberman, A. M., and M. J. Shlomchik. 2003. Reassessing the function of immune-complex retention by follicular dendritic cells. *Nat. Rev. Immunol. 3:757*.
32. Livak, K. J., and T. D. Schmittgen. 2001. Analysis of relative gene expression data using real-time quantitative PCR and the 2(-ΔΔ C_T) method. *Methods 25:402*.
33. Jack, R. S., T. Imanishi-Kari, and K. Rajewsky. 1977. Idiotypic analysis of the response of C57BL/6 mice to the (4-hydroxy-3-nitrophenyl)acetyl group. *Eur. J. Immunol. 7:559*.
34. Reth, M., G. J. Hammerling, and K. Rajewsky. 1978. Analysis of the repertoire of anti-NP antibodies in C57BL/6 mice by cell fusion. I. Characterization of antibody families in the primary and hyperimmune response. *Eur. J. Immunol. 8:393*.
35. Aydar, Y., J. Wu, J. Song, A. K. Szakal, and J. G. Tew. 2004. FcγRII expression on follicular dendritic cells and immunoreceptor tyrosine-based inhibition motif signaling in B cells. *Eur. J. Immunol. 34:98*.
36. Aydar, Y., P. Balogh, J. G. Tew, and A. K. Szakal. 2003. Altered regulation of FcγRII on aged follicular dendritic cells correlates with immunoreceptor tyrosine-based inhibition motif signaling in B cells and reduced germinal center formation. *J. Immunol. 171:5975*.
37. Chen, Z., S. B. Koralov, and G. Kelsoe. 2000. Regulation of humoral immune responses by CD21/CD35. *Immunol. Rev. 176:194*.
38. Aubry, J.-P., S. Pochon, P. Graber, K. Jansen, and J.-Y. Bonnefoy. 1992. CD21 is a ligand for CD23 and regulates IgE production. *Nature 358:505*.
39. Aydar, Y., P. Balogh, J. G. Tew, and A. K. Szakal. 2002. Age-related depression of FDC accessory functions and CD21 ligand-mediated repair of co-stimulation. *Eur. J. Immunol. 32:2817*.
40. Muramatsu, M., V. S. Sankaranand, S. Anant, M. Sugai, K. Kinoshita, N. O. Davidson, and T. Honjo. 1999. Specific expression of activation-induced cytidine deaminase (AID), a novel member of the RNA-editing deaminase family in germinal center B cells. *J. Biol. Chem. 274:18470*.
41. Muramatsu, M., K. Kinoshita, S. Fagarasan, S. Yamada, Y. Shinkai, and T. Honjo. 2000. Class switch recombination and hypermutation require activation-induced cytidine deaminase (AID), a potential RNA editing enzyme. *Cell 102:553*.
42. Faili, A., S. Aoufouchi, Q. Gueranger, C. Zober, A. Leon, B. Bertocci, J. C. Weill, and C. A. Reynaud. 2002. AID-dependent somatic hypermutation occurs as a DNA single-strand event in the BL2 cell line. *Nat. Immunol. 3:815*.
43. Berek, C., A. Berger, and M. Apel. 1991. Maturation of the immune response in germinal centers. *Cell 67:1121*.
44. Kraal, G., I. L. Weissman, and E. C. Butcher. 1985. Germinal center cells: antigen specificity, heavy chain class expression and evidence of memory. *Adv. Exp. Med. Biol. 186:145*.
45. Tsiagbe, V. K., P. J. Linton, and G. J. Thorbecke. 1992. The path of memory B-cell development. *Immunol. Rev. 126:113*.
46. Jacob, J., G. Kelsoe, K. Rajewsky, and U. Weiss. 1991. Intraclonal generation of antibody mutants in germinal centres. *Nature 354:389*.
47. Tew, J. G., T. E. Mandel, and A. W. Burgess. 1979. Retention of intact HSA for prolonged periods in the popliteal lymph nodes of specifically immunized mice. *Cell. Immunol. 45:207*.
48. Tew, J. G., and T. E. Mandel. 1978. The maintenance and regulation of serum antibody levels: evidence indicating a role for antigen retained in lymphoid follicles. *J. Immunol. 120:1063*.
49. Kinoshita, K., J. Tashiro, S. Tomita, C. G. Lee, and T. Honjo. 1998. Target specificity of immunoglobulin class switch recombination is not determined by nucleotide sequences of S regions. *Immunity 9:849*.
50. Muto, T., M. Muramatsu, M. Taniwaki, K. Kinoshita, and T. Honjo. 2000. Isolation, tissue distribution, and chromosomal localization of the human activation-induced cytidine deaminase (AID) gene. *Genomics 68:85*.
51. Fang, Y., C. Xu, Y. X. Fu, V. M. Holers, and H. Molina. 1998. Expression of complement receptors 1 and 2 on follicular dendritic cells is necessary for the generation of a strong antigen-specific IgG response. *J. Immunol. 160:5273*.
52. Molina, H., V. M. Holers, B. Li, Y. Fung, S. Mariathasan, J. Goellner, J. Strauss-Schoenberger, R. W. Karr, and D. D. Chaplin. 1996. Markedly impaired humoral immune response in mice deficient in complement receptors 1 and 2. *Proc. Natl. Acad. Sci. USA 93:3357*.